Mutations in *SCN3A* Cause Early Infantile Epileptic Encephalopathy

Tariq Zaman, PhD,[1] Ingo Helbig, MD,[1,2,3] Ivana Babić Božović, MD, PhD,[4] Suzanne D. DeBrosse, MD,[5] A. Christina Bergqvist, MD,[1] Kimberly Wallis, LCGC,[5] Livija Medne, MS, LCGC,[6] Aleš Maver, MD, PhD,[7] Borut Peterlin, PhD,[7] Katherine L. Helbig, MS, LCGC,[1,8] Xiaohong Zhang, PhD,[1] and Ethan M. Goldberg, MD, PhD[1,3,9]

Objective: Voltage-gated sodium (Na^+) channels underlie action potential generation and propagation and hence are central to the regulation of excitability in the nervous system. Mutations in the genes *SCN1A*, *SCN2A*, and *SCN8A*, encoding the Na^+ channel pore-forming (α) subunits Nav1.1, 1.2, and 1.6, respectively, and *SCN1B*, encoding the accessory subunit β_1, are established causes of genetic epilepsies. *SCN3A*, encoding Nav1.3, is known to be highly expressed in brain, but has not previously been linked to early infantile epileptic encephalopathy. Here, we describe a cohort of 4 patients with epileptic encephalopathy and heterozygous de novo missense variants in *SCN3A* (p.Ile875Thr in 2 cases, p.Pro1333Leu, and p.Val1769Ala).
Methods: All patients presented with treatment-resistant epilepsy in the first year of life, severe to profound intellectual disability, and in 2 cases (both with the variant p.Ile875Thr), diffuse polymicrogyria.
Results: Electrophysiological recordings of mutant channels revealed prominent gain of channel function, with a markedly increased amplitude of the slowly inactivating current component, and for 2 of 3 mutants (p.Ile875Thr and p.Pro1333Leu), a leftward shift in the voltage dependence of activation to more hyperpolarized potentials. Gain of function was not observed for Nav1.3 variants known or presumed to be inherited (p.Arg1642Cys and p.Lys1799Gln). The antiseizure medications phenytoin and lacosamide selectively blocked slowly inactivating over transient current in wild-type and mutant Nav1.3 channels.
Interpretation: These findings establish *SCN3A* as a new gene for infantile epileptic encephalopathy and suggest a potential pharmacologic intervention. These findings also reinforce the role of Nav1.3 as an important regulator of neuronal excitability in the developing brain, while providing additional insight into mechanisms of slow inactivation of Nav1.3.

ANN NEUROL 2018;00:000–000

Voltage-gated sodium (Na^+) channels mediate the generation and propagation of electrical signals in excitable tissues including brain, spinal cord and peripheral nerve, and muscle.[1–3] Sodium channels are composed of a pore-forming α and auxiliary β subunits. In mammals, 9 α subunits (Nav1.1–1.9) have been identified (encoded by the genes *SCN1A–5A* and *SCN8A–11A*).[4] These α subunits consist of 4 domains (I–IV), each with 6 transmembrane segments (S1–S6), with S1–S4 forming the voltage sensor and S5–S6 of each domain contributing to the central ion-conducting pore.[1] Mutation of sodium channels is a known cause of abnormal excitability underlying human disease including epilepsy, cardiac arrhythmia, periodic paralysis, and pain syndromes.[2] Interestingly, all voltage-gated sodium channels, except Nav1.3, have known, well-established human disease associations.

View this article online at wileyonlinelibrary.com. DOI: 10.1002/ana.25188

Received Nov 17, 2017, and in revised form Feb 1, 2018. Accepted for publication Feb 18, 2018.

Address correspondence to Dr Goldberg, Children's Hospital of Philadelphia, Abramson Research Center, Room 502A, Philadelphia, PA 19104. E-mail: goldberge@email.chop.edu

From the [1]Division of Neurology, Department of Pediatrics, Children's Hospital of Philadelphia, Philadelphia, PA; [2]Department of Neuropediatrics, University Medical Center Schleswig-Holstein, Christian Albrecht University, Kiel, Germany; [3]Department of Neurology, Perelman School of Medicine, University of Pennsylvania, Philadelphia, PA; [4]Department of Biology and Medical Genetics, School of Medicine, University of Rijeka, Rijeka, Croatia; [5]Departments of Genetics and Genome Sciences, Pediatrics, and Neurology, and Center for Human Genetics, Case Western Reserve University School of Medicine, Cleveland, OH; [6]Division of Human Genetics, Department of Pediatrics, Individualized Medical Genetics Center, Children's Hospital of Philadelphia, Philadelphia, PA; [7]Clinical Institute of Medical Genetics, University Medical Centre Ljubljana, Ljubljana, Slovenia; [8]Division of Clinical Genomics, Ambry Genetics, Aliso Viejo, CA; and [9]Department of Neuroscience, Perelman School of Medicine, University of Pennsylvania, Philadelphia, PA

TABLE 1. Epilepsy-Associated Nav1.3 Mutant Channels: Present Report

Patient	Amino Acid Change	Domain	Segment	Inheritance Pattern	Epilepsy Age of Onset	EEG Classification	Seizure Semiology	DD	MRI
1	p.I875T	2	4–5 linker	De novo	2 wk	Multifocal	Tonic or myoclonic motor onset	Profound	PMG
2	p.I875T	2	4–5 linker	De novo	2 wk	Multifocal	Tonic or generalized tonic–clonic motor onset	Profound	PMG
3	p.P1333L	3	4–5 linker	De novo	1–3 days	Hypsarrhythmia; multifocal	Tonic, focal motor	Severe	NA
4	p.V1769A	4	6	De novo	<1 yr	Multifocal	NA	Yes	NA
5	p.R1642C	4	5	Unknown[a]	18 mo	NA	Focal onset with impaired awareness	Yes	Normal

[a]Nonmaternal; father not available for testing.
DD = developmental delay; EEG = electroencephalographic; MRI = magnetic resonance imaging; NA = not available for review; PMG = polymicrogyria.

The predominant Na^+ channels expressed in brain are Nav1.1, 1.2, 1.3, and 1.6.[1] Mutations in the genes encoding 3 of these 4 channels are highly associated with epilepsy; heterozygous loss of function mutation of *SCN1A* (encoding Nav1.1) is the major cause of Dravet syndrome spectrum disorders.[5,6] Mutations of *SCN2A*[7–9] (encoding Nav1.2) and *SCN8A*[10,11] (encoding Nav1.6) are also well-established causes of genetic epilepsy, associated with a wider phenotypic spectrum that includes early infantile epileptic encephalopathy. However, a link between Nav1.3 and epilepsy has been less clear.

SCN3A encodes the type 3 voltage-gated Na^+ channel α subunit Nav1.3, which is known to be highly expressed in embryonic brain.[12,13] Postnatal expression levels in rodents is low or undetectable,[14,15] although Nav1.3 is upregulated in response to various insults to the nervous system including nerve injury[16,17] and in some rodent models of epilepsy.[18,19] However, Nav1.3 knockout mice appear healthy.[16] A specific function of Nav1.3 in brain is not clear. However, it has been consistently noted that Nav1.3 current includes a relatively prominent slowly inactivating/"persistent" current component (I_{NaP}) of between 0.5 and 10.3% of peak transient sodium current (I_{NaT}).[20–22]

Previous studies have reported heterozygous variants in *SCN3A* in association with less severe forms of epilepsy; [21–25] however, de novo mutation in *SCN3A* as a cause of early infantile epileptic encephalopathy has yet to be described. Prior reports include cases of focal epilepsy, with onset after infancy, and not consistently associated with developmental delay/intellectual disability; variants were in most instances not shown definitively to be de novo mutations. Here, we describe a cohort of 4 patients with infantile onset epileptic encephalopathy due to verified de novo mutation of *SCN3A*, and characterize the functional consequences of these mutations electrophysiologically. We also assess the electrophysiological properties of 2 *SCN3A* variants that were either demonstrated or suspected to be inherited. These latter variants did not show the gain of function seen in patients with a proven de novo mutation and early infantile epileptic encephalopathy. Our results support the status of *SCN3A* as an early infantile epileptic encephalopathy gene and further suggest that the mechanism of severe epilepsy is gain of function; our results show a prominent increase in I_{NaP} and, for 2 of the 3 mutants, an apparent leftward shift in the voltage dependence of channel activation.

Subjects and Methods

Study Subjects

Patients included in the study (Table 1) were either seen and evaluated at the Children's Hospital of Philadelphia (Philadelphia, PA), the University Hospitals Cleveland Medical Center (Cleveland, OH), or the Clinical Institute of Medical Genetics, University Medical Centre Ljubljana (Ljubljana, Slovenia), or were ascertained through a collaboration with Ambry Genetics (Aliso Viejo, CA). Informed consent was obtained from all parent(s) where applicable. This study was approved by the local institutional review boards at each of the participating

centers. All patients were unrelated, and pregnancy and birth history were unremarkable for all patients.

Patient 1 was a male with epilepsy onset at age 2 weeks, with continued intractable epilepsy at last follow-up (at age 13 years), accompanied by microcephaly, profound global developmental delay, and central hypotonia. There were multiple seizure types including tonic and myoclonic seizures. At last follow-up, the patient remained nonverbal and nonambulatory, with dysphagia and failure to thrive requiring exclusive feeding via gastrostomy tube. Magnetic resonance imaging (MRI) of the brain showed extensive frontoparietal polymicrogyria with thickening of the cerebral cortex. Trio whole exome sequencing (WES) analysis revealed a de novo heterozygous c.2624T>C missense mutation in *SCN3A* leading to an p.Ile875Thr amino acid substitution (based on National Center for Biotechnology Information Reference Sequence NP_008853.3 for human Nav1.3 isoform 1; see below).

Patient 2 was a female born at term after an uncomplicated pregnancy and delivery, with onset of seizures at age 2 weeks that were described as generalized tonic. MRI of the brain showed diffuse, bilateral polymicrogyria, abnormal white matter, and thin corpus callosum. The patient was also found to have a de novo c.2624T>C missense mutation leading to a p.Ile875Thr amino acid substitution. As of last follow-up, at age 3 years, the patient exhibited severe global developmental delay, central hypotonia, spastic tetraparesis, and intractable epilepsy.

Patient 3, a male born at full term, had onset of seizures on day of life 1 (36 hours), characterized by bradycardia, oxygen desaturation, and tonic unilateral upper extremity movements. An initial electroencephalogram (EEG) performed at age 2 weeks showed hypsarrhythmia, with high-amplitude multifocal epileptiform discharges along with eye deviation or tonic unilateral limb movements associated with electrodecrement; classical flexor or extensor spasms were not noted. Repeat EEG at age 6 months showed multifocal sharp waves and spikes and multifocal areas of intermittent slowing. Epilepsy remained refractory to treatment at last follow-up at approximately 2 years of age, at which time the patient exhibited severe global developmental delay, central hypotonia, and cortical blindness. Seizure types included unilateral clonic or tonic–clonic movements of an extremity, ipsilateral facial twitching, and/or upward or lateral eye deviation. MRI of the brain showed thinning of the corpus callosum and low–normal myelination of the cerebral white matter; head circumference was normal. WES revealed a de novo heterozygous c.3998C>T missense mutation in *SCN3A* leading to a p.Pro1333Leu amino acid substitution.

Patient 4, a female, had epilepsy onset within the first year of life, although exact age of onset is unknown. There was continued developmental delay and intractable epilepsy at age 4 years. EEG showed multifocal epileptiform discharges. WES demonstrated a de novo c.5306T>C missense mutation in *SCN3A* leading to a Val1769Ala amino acid substitution. MRI of the brain was not performed.

Patient 5, a male, had normal early childhood development, with epilepsy onset at 18 months. Epilepsy became intractable by age 3 years, with developmental arrest and regression of speech/language and motor development. At last follow-up at age 32 years, the patient continued to suffer from intractable epilepsy with minimal independent ambulation and severe intellectual impairment. Seizures have been of apparent focal onset, with arrest of activity and staring, sometimes progressing to limb stiffening and occasional falling. MRI of the brain was normal, showing only a likely posterior fossa arachnoid cyst. Neurological examination was significant for low axial tone and peripheral spasticity. WES revealed a c.4924C>T missense variant leading to a p.Arg1642Cys substitution in *SCN3A* that was shown to be not inherited from the patient's mother; however, the inheritance pattern could not be strictly established, as the patient's biological father was not available for testing.

Patient 6 had onset of infantile spasms at age 4 months accompanied by developmental arrest. By age 17 years, the patient exhibited severe intellectual impairment and was nonverbal, with ataxic gait, continued seizures, and a hyperkinetic movement disorder. WES analysis revealed a c.5395A>C variant in *SCN3A* leading to a p.Lys1799Gln amino acid substitution in Nav1.3 that was subsequently shown to be maternally inherited and was hence considered a variant of uncertain significance.

Exome analysis in all cases included more detailed evaluation of variants in genes associated with developmental delay, epilepsy, and brain malformation. All variants in *SCN3A* were confirmed via Sanger sequencing.

Cell Culture, Plasmid Preparation, and Transfection

Transfections and electrophysiological experiments were performed using tsA-201 cells. Cells were grown at 37 °C with 5% CO_2 in Dulbecco modified Eagle medium (DMEM) supplemented with 10% fetal bovine serum, 2mM L-glutamine, and penicillin (50 U/mL)–streptomycin (50 μg/ml).

A plasmid encoding the major splice isoform of human *SCN3A* (isoform 2, which is 49 amino acids longer than isoform 1) was used (Reference Sequence NP_001075145.1), and variants were introduced by site-directed mutagenesis. Constructs were propagated in STBL2 cells at 30 °C (Invitrogen, Carlsbad, CA). All plasmid preparations were resequenced prior to transfection. Plasmids encoding human sodium channel auxiliary subunits β_1 (hβ_1-V5-2A-dsRed) or β_2 (pGFP-IRES- hβ2) were cotransfected in vectors containing marker genes facilitating the identification of cells expressing all 3 constructs (Nav1.3, Navβ_1, and Navβ_2). We performed transient transfection of 2 μg total cDNA at a ratio of Nav1.3, β_1, and β_2 of 10:1:1 using Lipofectamine 2000 (Invitrogen) transfection reagent. Cells were incubated for 48 hours after transfection prior to electrophysiological recording. Transfected cells were dissociated by brief exposure to trypsin/ethylenediaminetetraacetic acid, resuspended in supplemented DMEM medium, plated on 15mm glass coverslips, and allowed to recover for at least 4 hours at 37 °C in 5% CO_2 prior to recording.

Electrophysiology

Glass coverslips were placed in a chamber housed on the stage of an upright epifluorescence microscope for electrophysiological recording. Extracellular solution contained, in mM: NaCl, 145; KCl, 4.0; $CaCl_2$, 1.8; $MgCl_2$, 1.8; hydroxyethylpiperazine ethane sulfonic acid (HEPES), 10. pH was adjusted to 7.35 with NaOH. Intracellular pipette-filling solution contained, in mM: CsF, 110; NaF, 10; CsCl, 20; ethyleneglycoltetraacetic acid, 2.0; HEPES, 10. pH was adjusted to 7.35 with CsOH and osmolarity to 305mOsm/l with sucrose. All chemicals were produced by Sigma-Aldrich (St Louis, MO). Recordings were performed using an agar bridge (2% in extracellular solution) reference electrode.

Recording pipettes were fashioned from thin-walled borosilicate glass (Sutter Instruments, Novato, CA) using a 2-stage upright puller (PC-10; Narishige, Tokyo, Japan), fire-polished using a microforge (MF-830, Narishige), and coated with Sylgard 182 (Dow Corning, Midland, MI). The resistance of pipettes when placed in extracellular solution was 2.18 ± 0.04MΩ. Cells that were positive for both red fluorescent protein (β_1 expression) and green fluorescent protein (β_2 expression) and exhibited fast transient inward current consistent with a voltage-gated sodium current were selected for subsequent analysis.

Whole cell patch clamp recordings were performed at room temperature (22–24 °C) using a MultiClamp 700B amplifier (Molecular Devices, Sunnyvale, CA). Pipette capacitance was zeroed after formation of a gigaseal. Access resistance was 4.75 ± 0.16MΩ, and recording was initiated after 10 minutes of equilibration, after which recorded currents were found to be stable, and voltage errors were reduced via partial series resistance compensation. Voltage clamp pulses were generated using Clampex 10.6, acquired at 10kHz, and filtered at 5kHz. Leak was subtracted either using a standard P/4 protocol or post hoc using a similar method involving a small prepulse. Cells were rejected from analysis if access resistance changed >15% during the recording.

The activation protocol was performed using 20-millisecond steps from a holding potential of −120mV to potentials ranging from −80mV to a maximum of 50mV, in 5mV increments, with a 10-second intersweep interval. Current was converted to current density (pA/pF) by normalizing to cell capacitance. Conductance was derived using $G = I / (V - E_{Na})$, where G is conductance, I is current, V is voltage, and E_{Na} is the calculated equilibrium potential for sodium (+68.0mV). Conductance was normalized to maximum conductance, which was fit with a Boltzmann function to determine the voltage at half-maximal channel activation ($V_{1/2}$ of activation) and slope factor k. Persistent current was measured as the average value of the current response in the last 10 milliseconds of a 200-millisecond test pulse to −10mV. The prepulse voltage dependence was determined using a 100-millisecond prepulse to various potentials from a holding potential of −120mV, followed by a 20-millisecond test pulse to −10mV. Normalized conductance was plotted against voltage and fit with a Boltzmann function to determine the voltage at half-maximal inactivation ($V_{1/2}$ of inactivation) and slope factor k. Kinetics of recovery from channel inactivation was determined using a 1-second prepulse to −10mV from a holding potential of −120mV followed by a variable time delay to a 10-millisecond test pulse to −10mV. Data were fit with a double exponential function to determine the first (τ_1) and second (τ_2) time constants of recovery and their relative weights.

Ramp currents were obtained using a voltage ramp from −120 to + 40mV at 0.8mV/ms. Peak current and total charge (area under the curve; in Coulombs) were calculated.

Pharmacologic experiments were performed via bath perfusion. 5,5-Diphenylhydantoin (phenytoin) was from Sigma-Aldrich. Lacosamide (L098500) was purchased from Toronto Research Chemicals (Toronto, Ontario, Canada), dissolved in methanol, and stored as 100mM stock solution prior to 1:1,000 dilution in extracellular solution. For such experiments, control extracellular solution contained the same final concentration of methanol (0.0998%).

All recordings and data analysis were performed blind to experimental group.

Data Analysis

Data for standard electrophysiological parameters were obtained from at least n = 12 cells (1 from each coverslip) from at least 6 separate transfections for each experiment. Data were analyzed using Clampfit 10.6 (Molecular Devices) or using custom scripts written in MATLAB (MathWorks, Natick, MA), and statistics were generated and plotted using Statistical Package for the Social Sciences version 14 (SPSS, Chicago, IL), Microsoft Excel (Microsoft, Redmond, WA), Prism (GraphPad Software, La Jolla, CA), and Sigma Plot 11 (Systat Software, San Jose, CA). Results are presented as the mean ± standard error of the mean, and statistical significance was established using the p value calculated from a paired or unpaired Student t test, or via 1-way analysis of variance (ANOVA) with Bonferroni correction for multiple comparisons, as appropriate, with the p value specified at the $p < 0.05$, 0.01, or 0.001 level, or reported exactly.

Results

We identified a cohort of 4 patients with severe infantile onset epileptic encephalopathy and de novo heterozygous variants in *SCN3A* encoding the type 3 voltage-gated Na^+ channel α subunit Nav1.3 (Fig 1, Table 1). Two of the patients (Patients 1 and 2) carried the same de novo p.Ile875Thr variant, whereas the other 2 patients harbored unique de novo variants p.Pro1333Leu and p.Val1769Ala. We also included 2 patients with *SCN3A* variants that were presumed (Patient 5) or demonstrated to be inherited (Patient 6). The 4 patients (Patients 1–4) with confirmed de novo mutation had intractable epilepsy with onset during infancy and severe to profound developmental delay. MRI of the brain was essentially normal in all cases except for the 2 patients with

A

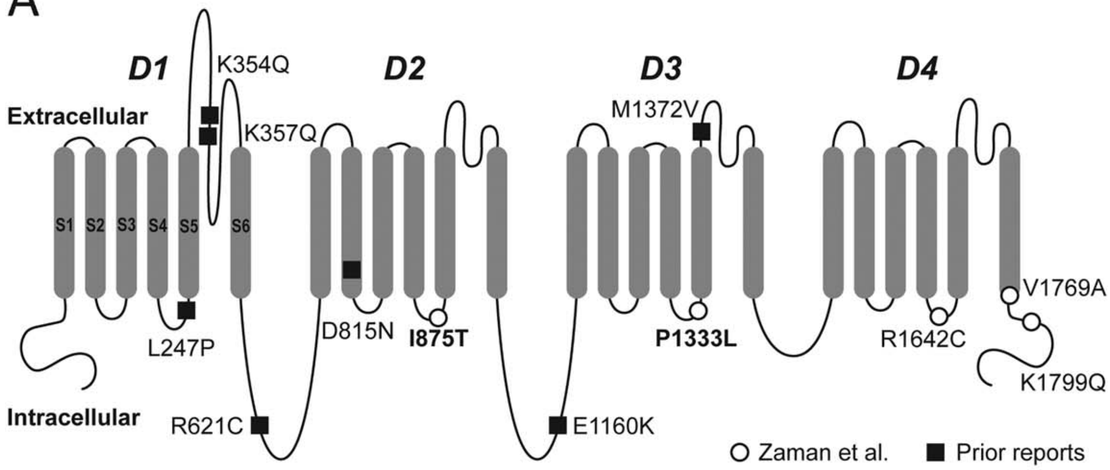

B

Patients 1 & 2 - I875T

		T (above residue 875 in isoform 1)	
Brown bat	860	L R S F R L L R V F R L A K S W P T L N M L I K I I G N S V G A L	893
Garter snake	846	L R S F R L L R V F R L A K S W P T L N M L I K I I G N S V G A L	879
Cuckoo	860	L R S F R L L R V F R L A K S W P T L N M L I K I I G N S V G A L	893
Mouse Scn3a	811	L R S F R L L R V F R L A K S W P T L N M L I K I I G N S V G A L	844
Human Nav1.1	846	L R S F R L L R V F R L A K S W P T L N M L I K I I G N S V G A L	879
Human Nav1.3 (isoform 1)	850	L R S F R L L R V F R L A K S W P T L N M L I K I I G N S V G A L	883
Human Nav1.3 (isoform 2/3)	801	L R S F R L L R V F R L A K S W P T L N M L I K I I G N S V G A L	834
		* *	

Patient 3 - P1333L

		L	
Brown bat	1311	L R T L R A L R P L R A L S R F E G M R V V V N A L I G A I P S I	1344
Garter snake	1303	L R T L R A L R P L R A L S R F E G M R V V V N A L V G A I P S I	1336
Cuckoo	1317	L R T L R A L R P L R A L S R F E G M R V V V N A L V G A I P S I	1350
Mouse Scn3a	1255	L R T L R A L R P L R A L S R F E G M R V V V N A L V G A I P S I	1288
Human Nav1.1	1314	L R T L R A L R P L R A L S R F E G M R V V V N A L L G A I P S I	1347
Human Nav1.3 (isoform 1)	1302	L R T L R A L R P L R A L S R F E G M R V V V N A L V G A I P S I	1335
Human Nav1.3 (isoform 2/3)	1253	L R T L R A L R P L R A L S R F E G M R V V V N A L V G A I P S I	1286
		* : * * * * * *	

Patient 4 - V1769A

		A	
Brown bat	1758	F F V S Y I I I S F L V V V N M Y I A V I L E N F S V A T E E S A	1799
Garter snake	1753	F F V S Y I I I S F L V V V N M Y I A V I L E N F S V A T E E S A	1794
Cuckoo	1767	F F V S Y I I I S F L V V V N M Y I A V I L E N F S V A T E E S A	1808
Mouse Scn3a	1701	F F V S Y I I I S F L V V V N M Y I A V I L E N F S V A T E E S A	1734
Human Nav1.1	1764	F F V S Y I I I S F L V V V N M Y I A V I L E N F S V A T E E S A	1797
Human Nav1.3 (isoform 1)	1749	F F V S Y I I I S F L V V V N M Y I A V I L E N F S V A T E E S A	1782
Human Nav1.3 (isoform 2/3)	1700	F F V S Y I I I S F L V V V N M Y I A V I L E N F S V A T E E S A	1733
		* *	

Patient 5 - R1642C

		C	
Brown bat	1628	T L F R V I R L A R I G R I L R L I K G A K G I R T L L F A L M M	1669
Garter snake	1623	T L F R V I R L A R I G R I L R L I K G A K G I R T L L F A L M M	1664
Cuckoo	1637	T L F R V I R L A R I G R I L R L I K G A K G I R T L L F A L M M	1678
Mouse Scn3a	1571	T L F R V I R L A R I G R I L R L I K G A K G I R T L L F A L M M	1602
Human Nav1.1	1634	T L F R V I R L A R I G R I L R L I K G A K G I R T L L F A L M M	1665
Human Nav1.3 (isoform 1)	1619	T L F R V I R L A R I G R I L R L I K G A K G I R T L L F A L M M	1650
Human Nav1.3 (isoform 2/3)	1570	T L F R V I R L A R I G R I L R L I K G A K G I R T L L F A L M M	1603
		* *	

FIGURE 1: Locations of epilepsy-associated Nav1.3 variants. (A) Shown is a schematic of the Nav1.3 voltage-gated Na^+ channel α subunit, with domains (D) 1 to 4, and transmembrane segments (S) 1 to 6 (shown for D1). Epilepsy-associated variants previously reported in the literature are shown as closed squares, and those described in the present report are shown as open circles. Variants in bold are recurrent. Amino acid location is based on Reference Sequence NP_008853.3 (hNav1.3 isoform 1). (B) Nav1.3 mutations associated with epileptic encephalopathy occur at highly conserved amino acid residues, as shown using ClustalX multiple sequence alignment of human Nav1.3 isoforms 1, 2, and 3, human Nav1.1 homolog, and various species orthologs. The Nav1.3 variants described in this report are indicated in bold above the corresponding amino acid residue. The highly conserved arginine residues of the S4 helix of the voltage sensor of Nav1.3 are indicated by the boxed regions. Notation indicates conservation across human Na^+ channel genes and between species: colon, strongly similar; asterisk, fully conserved.

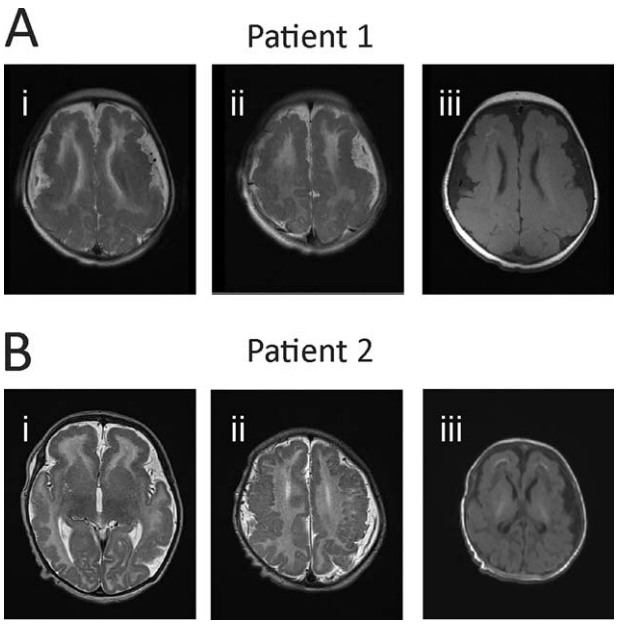

FIGURE 2: Magnetic resonance imaging (MRI) scans of patients with SCN3A-p.Ile875Thr mutation. (A) MRI for Patient 1. Axial T2 MRI images (Ai, Aii) at 2 rostrocaudal levels demonstrating extensive, bilaterally symmetric, predominantly frontoparietal polymicrogyria. There is incomplete opercularization of the insula with slightly dysplastic sylvian fissures. There are extensive foci of frontal subcortical and periventricular T1 shortening representing calcifications (Aiii). (B) MRI for Patient 2. Axial T2 MRI images (Bi, Bii) show diffuse polymicrogyria. T1 images show apparent subcortical calcifications in the frontal lobes (Biii).

p.Ile875Thr mutation (Patients 1 and 2; Fig 2). Previously reported cases of Nav1.3 variants associated with epilepsy are summarized for comparison (Table 2).

Na^+ channels are formed by a single polypeptide composed of 4 repeated domains (D1–D4), with each domain comprising 6 transmembrane segments (S1–S6); S1–S4 represent the voltage-sensing region, whereas S5–S6 forms the conducting pore. Identified variants in Patients 1–5 were in the S4–S6 domains (Tables 1 and 3). Figure 1B shows the sequence alignment between isoform 1 and isoforms 2 and 3 of hNav1.3 (see Subjects and Methods), between other human voltage-gated Na^+ channel α subunits, and across phylogeny. p.Ile875Thr identified in Patients 1 and 2 produces substitution of a hydrophobic isoleucine to polar uncharged threonine at a highly evolutionarily conserved residue located in the S4–S5 linker of D2. The p.Pro1333Leu mutation found in Patient 3 represents the substitution of a small, aliphatic amino acid proline by hydrophobic leucine at a residue located in the S4–S5 linker of D3 that is highly conserved between human Na^+ channels Nav1.1–1.9 as well as across phylogeny. The p.Val1769Ala mutation in Patient 4 results in substitution of an alanine for valine at a highly conserved residue in the S6 segment of D4. The p.Arg1642Cys variant of unknown inheritance detected in the more mildly affected Patient 5 produces a substitution of a positively charged arginine for cysteine at a conserved residue in the S4–S5 linker of D4.

Reference to in silico prediction software PolyPhen-2 and SIFT supports the pathogenic nature of the variants identified in the patients in the cohort with early infantile epileptic encephalopathy (Table 4). Variants were absent from control databases including the genome Aggregation Database and the Exome Variant Server. We also queried ClinVar for mutations in the other epilepsy-associated sodium channel genes *SCN1A, 2A*, and *8A* that were homologous to the *SCN3A* mutations reported here (Table 5) and determined that, for example, Nav1.1-p.Val1784Ala (an identical substitution at the position homologous to amino acid 1769 in Nav1.3) has

TABLE 2. Epilepsy-Associated Nav1.3 Variants in the Published Literature

Reference	Amino Acid Change	Inheritance Pattern	Epilepsy Age of Onset	Epilepsy Type	DD	MRI
Holland 2008[23]	p.Lys354Gln	Paternal	2 yr	Focal	No	Normal
Vanoye 2014[22]	p.Arg357Gln	Unknown	4 yr	Focal	Yes	Normal
Vanoye 2014[22]	p.Asp815Asn	Unknown	22 mo	Focal	Mild	Normal
Vanoye 2014[22]	p.Glu1160Lys	Unknown	Neonate	Focal	No	Normal
Vanoye 2014[22]	p.Met1372Val	Unknown	16 mo	FS; focal	No	Normal
Wang 2017[25]	p.Arg621Cys	Maternal	Unknown	FS; BECTS	No	Normal
Lamar 2017[24]	p.Leu247Pro	De novo	18 mo	Focal	Yes	Normal
Trujillano 2017[39]	p.Pro1333Leu	De novo	1–3 days	Unspecified	Severe	Normal

Note that all variants are presented in relation to Nav1.3 isoform 1 (Reference Sequence NP_008853.3).
BECTS = centrotemporal spikes on electroencephalogram; DD = developmental delay; FS = febrile seizures; MRI = magnetic resonance imaging.

TABLE 3. Biophysical Properties of WT Nav1.3 Channels and Nav1.3 Variants

	Current Density at −10mV		Voltage Dependence of Activation			Voltage Dependence of Inactivation			Recovery from Inactivation			Persistent Current	
	pA/pF	n	$V_{1/2}$, mV	*k*	n	$V_{1/2}$, mV	*k*	n	τ_1, ms	τ_2, ms	n	% of peak	n
WT	373.1 ± 16.8	27	−26.2 ± 1.3	5.1 ± 0.3	27	−69.7 ± 2.2	10.2 ± 1.2	9	3.9 ± 0.6	63.6 ± 20.9	4	2.6 ± 0.4	27
p.Ile875Thr	391.1 ± 28.6	15	−37.1 ± 1.4[a]	4.9 ± 0.5	14	−49.2 ± 6.4[b]	19.9 ± 3.2[b]	5	4.5 ± 1.5	47.6 ± 20.7	4	18.0 ± 3.5[a]	12
p.Pro1333Leu	384.4 ± 53.1	12	−37.7 ± 2.2[a]	4.7 ± 0.6	10	−58.7 ± 10.6	9.5 ± 1.3	4	2.6 ± 0.6	25.7 ± 4.4	6	10.7 ± 1.6[a]	14
p.Val1769Ala	364.1 ± 10.7	19	−29.4 ± 1.1	5.5 ± 0.3	27	−49.6 ± 3.9[c]	16.9 ± 2.1[b]	9	2.1 ± 0.1	71.5 ± 8.6	7	30.7 ± 2.8[a]	25
p.Arg1642Cys	360.9 ± 43.3	8	−21.6 ± 1.7	4.7 ± 0.5	6	−66.9 ± 1.7	4.9 ± 1.2[a]	5	1.2 ± 0.2[b]	26.4 ± 7.9	7	2.3 ± 0.4	12
p.V1799Q	344.9 ± 24.1	13	−24.7 ± 1.2	5.3 ± 0.4	13	−73.7 ± 2.1	7.8 ± 0.6	12	3.3 ± 0.4	49.5 ± 6.2	7	2.4 ± 0.7	13

[a]$p < 0.001$ versus WT (1-way analysis of variance with Bonferroni correction for multiple comparisons).
[b]$p < 0.05$ versus WT.
[c]$p < 0.01$ versus WT.
WT = wild type.

been reported in a patient with severe myoclonic epilepsy of infancy (SMEI; Dravet syndrome). A recent report of 9 patients with an early profound form of SMEI[26] reported 1 patient with an Nav1.1-p.Pro1345Ser mutation, an identical substitution at the amino acid residue homologous to position 1333 in *SCN3A* that is mutated in Patient 3 in our cohort. It should be noted that prior work has shown that homologous mutations in *SCN1A* and *3A* can have divergent effects on channel physiology.[27] Search of the online *SCN1A* database (http://www.molgen.ua.ac.be/SCN1AMutations/Home) revealed an additional case of a patient with genetic epilepsy with febrile seizures plus (GEFS+) due to familial p.Arg1657Cys missense mutation,[28,29] an identical amino acid substitution at the position homologous to residue 1642 in Nav1.3 that was identified in Patient 5.

To assess the functional effects of these variants, we performed whole cell voltage-clamp electrophysiological recordings of wild-type hNav1.3 and mutant hNav1.3 expressed in tsA-201 cells coexpressed with wild-type human β_1 and β_2 auxiliary subunits. Representative rapidly activating and rapidly inactivating inward currents are shown (Fig 3A), along with plots of average current density versus voltage (see Fig 3B, Table 4). Peak current density was 374.1 ± 18.5pA/pF for wild type (n = 27); 391.1 ± 28.6pA/pF for p.Ile875Thr (n = 14), and 411.5 ± 55.5pA/pF for p.Pro1333Leu (n = 10), which was not different between groups ($p = 0.27$ and 0.20 for wild type vs p.Ile875Thr and p.Pro1333Leu, respectively). Rise time was also not statistically different between groups; time to peak current (in milliseconds) at −10mV was 0.82 ± 0.05 for wild type (n = 27),

TABLE 4. ClinVar[a] Entries for Homologous Variants in Other Epilepsy-Associated Sodium Channel Genes

	SCN1A			*SCN2A*			SCN8A		
	a.a.	Variants	Phenotype	a.a.	Variants	Phenotype	a.a.	Variants	Phenotype
p.Ile875Thr	871	N	NA	873	N	NA	867	N	NA
p.Pro1333Leu	1345	P1345S	SMEI	1335	N	NA	1325	N	NA
p.Val1769Ala	1784	V1784A	SMEI	1774	N	NA	1764	N	NA
p.Arg1642Cys	1657	N	NA	1647	R1647H	Nonspecific	1638	R1638H	Not provided
p.Lys1799Gln	1814	N	NA	1804	N	NA	1794	N	NA

[a]https://www.ncbi.nlm.nih.gov/clinvar.
a.a. = homologous amino acid residue; N = no; NA = not applicable; SMEI = severe myoclonic epilepsy of infancy (Dravet syndrome).

TABLE 5. Epilepsy-Associated Nav1.3 Mutant Channels: Present Report and Review of the Literature

Patient	Amino Acid Change	ExAc[a]		gnomAD[b]		PolyPhen-2	
		Allele Count	Allele Frequency	Allele Count	Allele Frequency	Score	Prediction
1–2	p.Pro1333Leu	0	—	0	—	1.000	Probably damaging
3	p.Ile875Thr	0	—	0	—	1.000	Probably damaging
4	p.Val1769Ala	0	—	0	—	0.999	Probably damaging
5	p.Arg1642Cys	0	—	2/277,136	0.000007	1.000	Probably damaging
Holland 2008[23]	p.Lys354Gln	0	—	0	—	0.999	Probably damaging
Vanoye 2014[22]	p.Arg357Gln	8/121,404	0.000066	14/277,216	0.000051	0.003	Benign
Vanoye 2014	p.Asp815Asn	2/121,172	0.000017	4/274,730	0.000015	0.984	Probably damaging
Vanoye 2014	p.Glu1160Lys	2/121,302	0.000016	6/276,996	0.000022	0.996	Probably damaging
Vanoye 2014	p.Met1372Val	1/121,392	0.000008	7/277,124	0.000025	0.003	Benign
Wang 2017[25]	p.Arg621Cys	0	—	0	—	1.00	Probably damaging
Lamar 2017[24]	p.Leu247Pro	0	—	0	—	1.00	Probably damaging

[a]Exome Aggregation Consortium (http://exac.broadinstitute.org/).
[b]Genome Aggregation Database (http://gnomad.broadinstitute.org/).

0.75 ± 0.08 for Nav1.3-p.Ile875Thr ($n = 14$; $p = 0.43$ vs wild type via unpaired 2-tailed t test), 0.69 ± 0.06 for Nav1.3-p.Pro1333Leu ($n = 10$, $p = 0.18$), 0.74 ± 0.04 for Nav1.3-p.Val1769Ala ($n = 18$, $p = 0.32$), and 0.72 ± 0.05 for Nav1.3-p.Arg1642Cys ($n = 5$, $p = 0.43$).

Slightly higher peak current density values for p.Ile875Thr and p.Pro1333Leu are likely a consequence of a hyperpolarizing leftward shift in the voltage dependence of activation (see Fig 3B, C). In these 2 mutant channels, the voltage at which maximal inward current was observed was shifted in the hyperpolarized direction, being -15.9 ± 1.6mV for wild-type hNav1.3 ($n = 27$), -28.9 ± 2.4mV for p.Ile875Thr ($n = 14$, $p < 0.01$ vs wild type via 1-way ANOVA with Bonferroni correction for multiple comparisons), and -26.0 ± 2.8 for p.Pro1333Leu ($n = 10$, $p < 0.01$ vs wild type). In contrast, we did not observe a change in the voltage dependence of activation for Nav1.3-p.Val1769Ala (-17.6 ± 1.6, $n = 27$, $p = 0.079$ vs wild type via 1-way ANOVA).

We noted striking differences in the I_{NaP} between groups, defined here as residual noninactivating current at 200 milliseconds following a voltage step from -120mV (see Fig 3D–F). I_{NaP} was $2.6 \pm 0.4\%$ ($n = 27$) of I_{NaT} for wild-type channels, but was $17.9 \pm 3.4\%$ for p.Ile875Thr ($n = 12$, $p < 0.001$ vs wild type), $10.7 \pm 1.6\%$ for p.Pro1333Leu ($n = 14$, $p < 0.0001$ vs wild type), and $30.7 \pm 2.8\%$ for p.Val1769Ala ($n = 25$, $p < 0.0001$ vs wild type). We noted that this current was not persistent per se,[30–32] but rather inactivated with slow kinetics over the course of seconds for both wild-type and mutant Nav1.3 channels; for example, remaining current at 1 second following a voltage step to -10mV was $0.7 \pm 0.2\%$ of peak I_{NaT} for wild-type Nav1.3 channels ($n = 7$), and $5.3 \pm 1.4\%$ ($n = 7$) of peak for Nav1.3-p.Val1769Ala. We also found that Nav1.3-p.Val1769Ala mutant channels displayed markedly larger currents (wild type, 197.1 ± 26.0pA, $n = 7$; p.Val1769Ala, 1370.0 ± 305.0pA, $n = 12$; $p = 0.013$) and larger total charge (wild type, 0.96 ± 0.13 nanocoulomb [nC], $n = 7$; p.Val1769Ala, 9.0 ± 2.0nC, $n = 12$; $p = 0.012$) in response to 0.8mV/ms slow depolarizations (Fig 4C).

Targeting persistent current is a proposed therapeutic strategy in epilepsy.[33,34] As Nav1.3 mutants p.Ile875Thr, p.Pro1333Leu, and p.Val1769Ala showed increased persistent current relative to wild-type Nav1.3, we hypothesized that pharmacological agents that target I_{NaP} might normalize pathological epilepsy-associated Na^+ channel current, and could represent potential treatments for *SCN3A* encephalopathy. We tested agents known to exert activity on this current component. The I_{NaP} component of Nav1.3 has been shown to be blocked by various antiseizure medications including phenytoin, lacosamide, topiramate, and carbamazepine.[20,35] We first tested lacosamide, shown previously to act as a channel blocker primarily of Nav1.7,[35–37] but also of Nav1.3 and Nav1.8.[35]

Consistent with previous results from wild-type Nav1.3,[35] we found that 100 μM lacosamide had no effect on peak transient Na^+ current (before, 435.2 ± 24.4pA/pF; after, 447.4 ± 21.2pA/pF; n = 10, $p = 0.41$). We did find that lacosamide produced a small but statistically significant block of persistent current, as

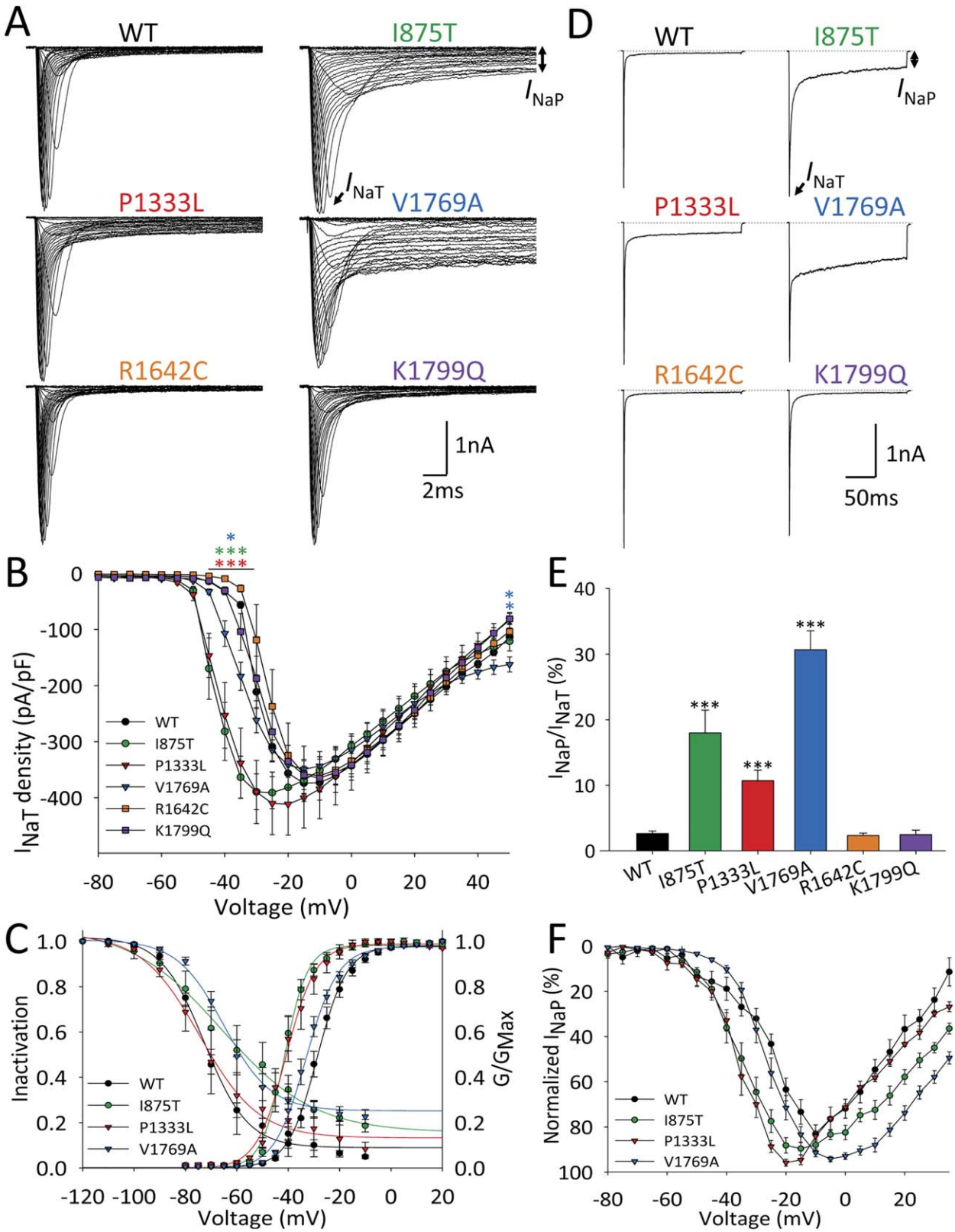

FIGURE 3.

measured at 200 milliseconds during a depolarizing pulse from −120 to −10mV (from 2.2 ± 1.0% to 0.8 ± 0.2% or 52.5 ± 6.9% block; n = 10, $p = 0.019$ via paired 2-tailed t test). This effect did not wash out; however, the effect was seen after an incubation time of as little as 1 minute. We confirmed that this purported block by lacosamide was not due to rundown of I_{NaP}, as persistent current was stable for at least 15 minutes in control experiments performed without addition of lacosamide to the extracellular solution.

We then tested lacosamide on heterologously expressed Nav1.3 mutants and found that it produced a similar proportional decrease in I_{NaP}. In Nav1.3-p.Val1769Ala mutants, which exhibit the largest persistent current, 100 μM lacosamide produced a 48.1 ± 5.1% block in I_{NaP}, from 33.0 ± 4.1% to 17.7 ± 2.8% of peak transient current (n = 10, $p < 0.001$). Similar effects (63.7 ± 1.2% block and 49.9 ± 6.7% block) were seen in p.Ile875Thr and p.Pro1333Leu mutants (see Fig 4A, B).

We next tested phenytoin, also known to block persistent sodium current.[30,38] In rat neocortical pyramidal neurons, phenytoin produces a hyperpolarizing shift in the voltage dependence of I_{NaP} inactivation.[30] One hundred micromolar phenytoin had a small effect on peak transient sodium current of wild-type Nav1.3 channels (control, 403.9 ± 34.7pA/pF; phenytoin, 318.5 ± 58.3pA/pF; n = 5, $p = 0.14$), but produced a decrease in I_{NaP} from 1.3 ± 0.3% to 0.8 ± 0.2% of peak transient current (n = 5, $p = 0.20$). In Nav1.3-p.Val1769Ala mutant channels, phenytoin also had minimal effect on I_{NaT} (control, 389.9.7 ± 36.7pA/pF; phenytoin, 365.7 ± 29.7pA/pF; n = 7, $p = 0.27$), but produced a striking reduction of I_{NaP} (from 24.0 ± 3.6% to 6.5 ± 0.9% of the transient current, a 68.4 ± 7.9% block; n = 7; $p = < 0.01$ via paired t test; see Fig 4C, D). Phenytoin also reduced peak currents (control, 3,002.6 ± 696.0pA; phenytoin, 1,149.0 ± 244.0pA; n = 5, $p = 0.026$) and total charge (control, 19.8 ± 4.7nC; phenytoin, 8.4 ± 2.0nC; n = 5, $p = 0.029$) in response to 0.8mV/ms slow ramp depolarizations from −120mV (see Fig 4C, D).

Discussion

Here we demonstrate that heterozygous missense mutations in the gene *SCN3A* encoding the voltage-gated Na^+ channel α subunit Nav1.3 are a cause of early infantile epileptic encephalopathy, identifying 3 causative variants in 4 patients. This conclusion is rigorously supported by multiple lines of evidence; the mutations are de novo and are absent from various control databases; the mutations occur at residues that exhibit a high level of evolutionary conservation; and functional studies demonstrate marked channel dysfunction. Mutations in other sodium channel genes *SCN1A, 2A*, and *8A*, encoding Nav1.1, 1.2, and 1.6, respectively, have been previously determined to be important causes of severe epilepsy with onset in early childhood. With this report, the 4 major neuronally expressed Na^+ channel genes have all been implicated as causes of early infantile epileptic encephalopathy.

By identifying patients with *SCN3A*-related early infantile epileptic encephalopathy (*SCN3A* encephalopathy), we extend prior reports that have linked *SCN3A* variants with milder forms of epilepsy. Holland et al reported a developmentally normal child with mild partial epilepsy onset at age 2 years with a heterozygous p.Lys354Gln variant in Nav1.3, which was inherited from the patient's unaffected father.[23] Estacion et al characterized rat *Scn3a* harboring the corresponding variant p.Lys343Gln ($rScn3a^{K343Q}$) in heterologous systems and found increased persistent current (from 4.4 ± 0.4% to 8.1 ± 1.4% of I_{NaT}).[21] Vanoye et al performed specific targeted sequencing of *SCN3A* in a cohort of epilepsy patients and reported 4 Nav1.3 variants associated with childhood onset epilepsy,[22] although none of the patients had early onset epileptic encephalopathy and inheritance pattern was not available. One variant, p.Glu1160Lys

FIGURE 3: Epilepsy-associated mutations alter function of the Nav1.3 channel. (A) Representative single leak-subtracted traces showing families of Na^+ currents elicited by 20-millisecond depolarizing voltage steps from −80 to + 50mV in 5mV increments from a holding potential of −120mV with a 10-second intersweep interval for wild type (WT) and each Nav1.3 variant coexpressed with β_1 and β_2. (B) Normalized *I-V* curves showing peak transient sodium current (I_{NaT}) density (in pA/pF) versus voltage for WT (n = 27), p.Ile875Thr (n = 14), p.Pro1333Leu (n = 10), p.Arg1642Cys (n = 8), p.Val1769Ala (n = 27), and p.Lys1799Gln (n = 13), presented as mean ± standard error of the mean. (C) Prepulse voltage-dependence of channel inactivation and conductance–voltage relationships for WT (n = 27), p.Ile875Thr (n = 14), p.Pro1333Leu (n = 10), and p.Val1769Ala (n = 19) were fit by a Boltzmann function. (D) Representative individual traces showing I_{NaT} and slowly inactivating/persistent current component (I_{NaP}) in response to a 200-millisecond voltage step from −120 to −10mV for WT Nav1.3 and p.Ile875Thr, p.Pro1333Leu, p.Arg1642Cys, p.Val1769Ala, and p.Lys1799Gln. (E) Bar graph showing ratio of I_{NaP}/I_{NaT} for WT (n = 27), p.Ile875Thr (n = 12), p.Pro1333Leu (n = 14), p.Arg1642Cys (n = 12), p.Val1769Ala (n = 25), and p.Lys1799Gln (n = 13), presented as mean ± standard error of the mean. (F) *I-V* curves of I_{NaP} in WT (n = 27) and Nav1.3 variants p.Ile875Thr (n = 14), p.Pro1333Leu (n = 10), and p.Val1769Ala (n = 13). Note that I_{NaP} at each voltage is normalized to the maximum value. *$p < 0.05$, **$p < 0.01$, ***$p < 0.001$ versus WT via 1-way analysis of variance with Bonferroni correction for multiple comparisons.

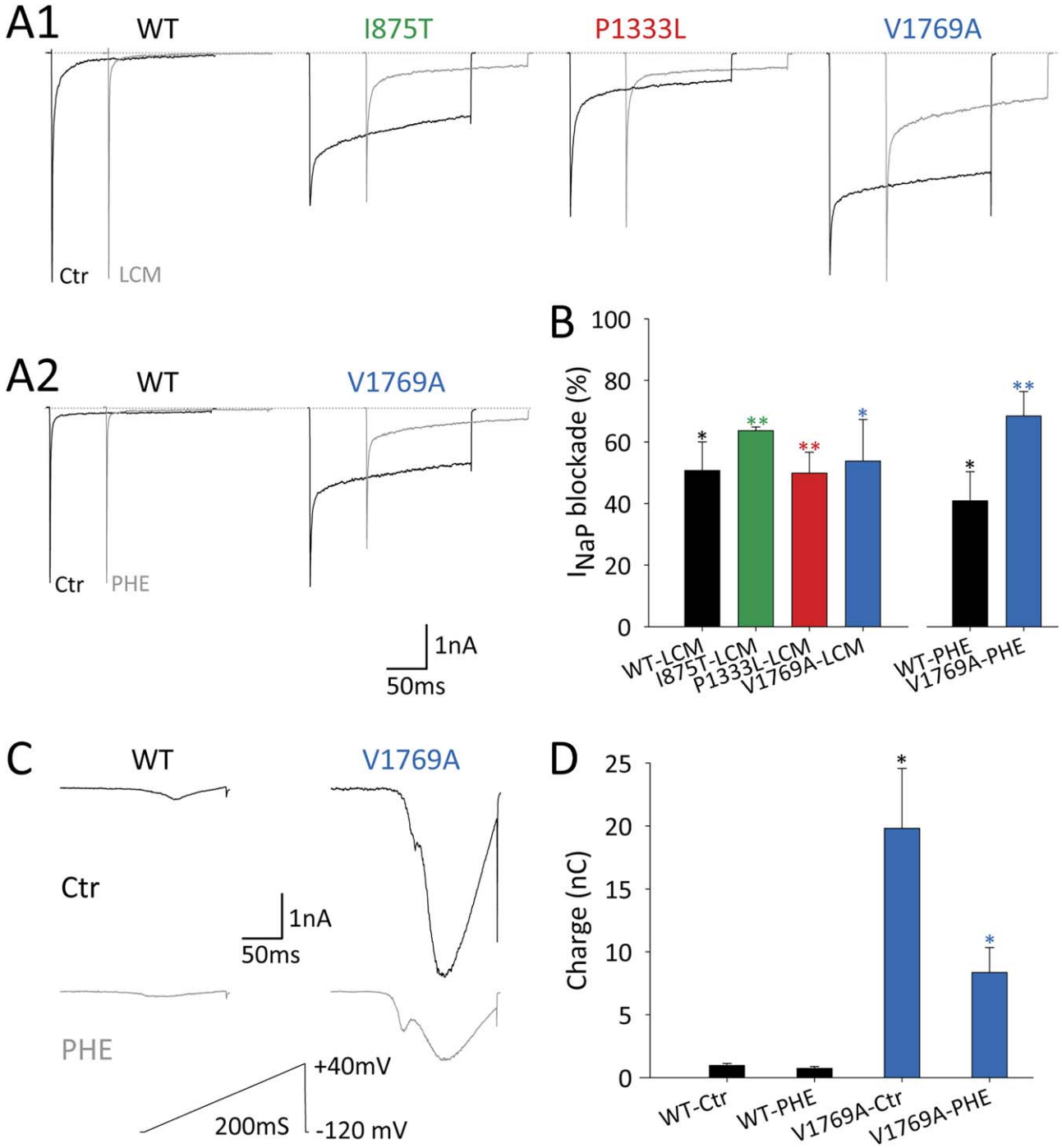

FIGURE 4: Antiseizure medications partially normalize pathological persistent current in Nav1.3 mutant channels. (A) Traces showing peak transient sodium current and slowly inactivating/persistent current component (I_{NaP}) of wild-type (WT) and mutant NaV1.3 channels before *(black traces)* and after *(gray traces)* application of 100 μM lacosamide (LCM; A1) and phenytoin (PHE; A2). (B) Bar graph showing percentage blockade of I_{NaP} by LCM (WT, n = 10; p.Ile875Thr, n = 6; p.Pro1333Leu, n = 6; p.Val1769Ala, n = 10) and PHE (WT, n = 3; p.Val1769Ala, n = 7). (C) Representative examples of Nav1.3 currents evoked by a voltage ramp from −120 to + 40mV at 0.8mV/ms in WT Nav1.3 (top left) and p.Val1769Ala mutant channels (top right), with block by PHE (bottom). (D) Quantification of charge (in nanocoulombs [nC]) between WT Nav1.3 (n = 5) and p.Val1769Ala (n = 5) before and after drug application. All data are presented as mean ± standard error of the mean. *$p < 0.05$, **$p < 0.01$ via paired 2-tailed *t* test.

(p.Glu1111Lys in hNav1.3 isoform 2), showed increased persistent current (1.2 ± 0.2% for p.Glu1111Lys versus 0.5 ± 0.1% for wild type). Lamar et al reported a patient with a de novo p.Leu247Pro mutation in Nav1.3 with developmental delay and focal epilepsy onset at 18 months[24]; functional studies showed decreased current density as well as cell surface expression suggesting loss of function. Trujillano et al reported a single patient with

febrile seizures and epilepsy with a de novo *SCN3A* p.Pro1333Leu mutation, which is the same mutation seen in Patient 3 in our study, although additional details regarding the patient phenotype were not provided.[39]

Taken together, the results of our study combined with previous investigations suggest a spectrum of *SCN3A*-related phenotypes, ranging from mild epilepsy with normal neurocognitive development to early infantile epileptic encephalopathy. Our study suggests that *SCN3A* mutations causative of epileptic encephalopathy exhibit prominent gain of function with markedly increased noninactivating Na^+ current, whereas variants identified in patients with milder phenotypes may result in loss of function or more subtle gain of function. For many of the previously reported cases of epilepsy associated with variants in *SCN3A*, inheritance could not be demonstrated, and such variants may represent rare population variants that could act as modifiers of disease or risk alleles rather than being causative of highly penetrant monogenic epilepsy per se.

Patients 1 and 2 in this study exhibited abnormal MRI showing polymicrogyria (see Fig 2). This was not a consistent feature of the cohort of patients with *SCN3A* encephalopathy, but was instead only seen in the two patients, who were unrelated, with the recurrent p.Ile875Thr variant, suggesting a potential mutation-specific effect on structural brain development. The basis of any association between *SCN3A* mutation and malformation of cerebral cortical development is unclear. Such an association could reflect a noncanonical ion channel function of Nav1.3, such as in mediating cell–cell interactions during cerebral cortical development, perhaps via interaction (or abnormal interaction) with or by auxiliary β subunits, which are known to have roles in cell adhesion. Alternatively, this could be due to an early deleterious effect of abnormal electrogenesis on neuronal migration and cerebral cortical development. It should be noted that we cannot absolutely rule out the unlikely possibility of a contribution of a second, perhaps somatic, mutation,[40] or mutation in an unknown gene, or of an early life insult such as infection or hypoxic ischemic brain injury, as contributory. Ascertainment of additional cases will be required to begin to clarify the issue of genotype:phenotype correlation and potential role of Nav1.3 in structural brain development. Of note, developmental brain malformations have also been found in patients with epilepsy with identified causative de novo mutations in other ion channels.[41,42]

Our findings offer the suggestion that *SCN3A* encephalopathy with onset in the first 2 months of life can be clearly differentiated from Dravet syndrome, which is mainly due to heterozygous loss of function of *SCN1A*.[5,6] This presumably reflects the differential developmental expression pattern of these two genes, with *SCN3A* being expressed at high levels during embryogenesis and during early postnatal life, falling to nearly undetectable levels by adulthood in rodent brain (although low-level expression persists in adult brain tissue[13]). In contrast, *SCN1A* expression is at low levels at birth, increasing in infancy and young childhood.[12]

The p.Ile875Thr and p.Pro1333Leu de novo mutations produce a marked leftward shift in the voltage dependence of activation of approximately 10mV. This finding is consistent with the location of these mutations in the S4–S5 linker, close to the positively charged arginine residues of the S4 helix domain of the voltage sensor. In addition, these mutations are located in D2 and 3, respectively: the first 3 domains are thought to be responsible for fast activation, which may account for the leftward shift in the voltage dependence of activation observed for these variants. The mutation identified in Patient 4 (p.Val1769Ala), which was not associated with a hyperpolarizing shift in the *G-V* curve (albeit smaller in magnitude), is located in D4.[43,44] Although the exact mechanism of voltage-dependent activation of Na^+ channels is not fully determined, it is thought that the S4–S5 linker translates voltage-dependent shifts of the S4 segment into opening of the pore,[45] with motion of S4–S5 coupled to that of neighboring S5 and S6 segments.[46]

We also found increased slowly inactivating/persistent current in p.Ile875Thr, p.Pro1333Leu, and p.Val1769Ala, corresponding to the 3 de novo mutations identified in the patients with early onset epileptic encephalopathy in this cohort. The persistent sodium current I_{NaP} remains a somewhat enigmatic feature of Na^+ channels and continues to be a subject of intense investigation. I_{NaP} is thought to be important for various cellular functions including regulation of repetitive firing and boosting of synaptic inputs, and in the generation of subthreshold membrane potential oscillations.[31,32,47,48] Nav1.3 is known to exhibit I_{NaP} in heterologous systems as well as in neurons under normal and pathological conditions.[21,49,50] The value for persistent current recorded here for wild-type Nav1.3 (2.6%) is higher that reported by Vanoye et al,[22] similar to that previously by Estacion et al,[21] and lower than reported by Sun et al.[20] This current may not be truly "persistent," but rather exhibits slow inactivation on the order of seconds or tens of seconds,[30,32,47,51–53] as we have also shown here. We further found that the antiseizure medications lacosamide and phenytoin selectively blocked I_{NaP} over I_{NaT} and that block was proportional to the amplitude of the persistent current.

Previous data indicate that mutations in various sodium channels across all 4 domains including intracellular loops could affect the amplitude of I_{NaP}.[54] The finding that Nav1.3-p.Ile875Thr (located in D2) and p.Val1769Ala (located in D4) were associated with the largest increase in I_{NaP} is consistent with a recent report using the tarantula toxin RTX-VII. This toxin increases Nav1.3-mediated I_{NaP} via interaction with D2 and D4.[55] Interestingly, focal application of RTX-VII to the surface of the cerebral cortex of adult rats induced seizures, consistent with a potentially ictogenic effect of increased Nav1.3 I_{NaP} and supporting the pathogenic mechanism proposed here. Why the p.Pro1333Leu mutation, located in D3, also increased I_{NaP}, remains unclear. Although additional work is required to further elucidate the structural basis of Nav1.3-mediated I_{NaP}, our results may provide some additional insight into this phenomenon.

We noted that the *I-V* relation of Na^+ channels containing Nav1.3-p.Val1769Ala exhibited a somewhat flat appearance at depolarized potentials. The basis of this observation is unclear and would require additional investigation, and may be attributable to allosteric modification of voltage-dependent gating by the Nav1.3-p.Val1769Ala mutation.

The inheritance pattern of the p.Arg1642Cys variant could not be definitively established. We did note that the p.Arg1642Cys variant is homologous to an p.Arg1657Cys missense mutation described in a family with GEFS+, and this difference between Dravet syndrome and the more mild GEFS parallels the difference in disease severity between Patient 5 and the more severe Patients 1–4 with proven de novo mutations. We did find that Nav1.3-p.Arg1642Cys channels appeared to recover from inactivation more rapidly, which might be predicted to increase neuronal excitability by supporting the ability to discharge action potentials repetitively. Further work will be required to better delineate the relationship of this variant to epilepsy and the mechanism whereby faster recovery from Na^+ inactivation might produce cellular hyperexcitability.

The establishment of a gene-specific diagnosis is important, as it may have current or future treatment implications. For example, clinical data indicate that epilepsy in patients with Dravet syndrome responds best to specific antiseizure medications, whereas antiseizure medications with a predominant mechanism of action of Na^+ channel blockade may exacerbate seizures and are considered to be contraindicated.[56,57] In contrast, recent reports suggest that epilepsy in some patients with *SCN8A* encephalopathy may respond well to sodium channel antagonists such as phenytoin.[7,58] Our data raise the possibility that early introduction of agents specifically targeting Nav1.3-mediated persistent Na^+ current, during the transient developmental time period within which this channel is expressed, represents a potential strategy for treatment of *SCN3A* encephalopathy.

In conclusion, we report a cohort of 4 patients with infantile onset epileptic encephalopathy due to de novo heterozygous gain-of-function missense mutations in the gene *SCN3A* encoding the type 3 voltage-gated sodium channel Nav1.3. Mutant channels exhibited various mechanisms of gain of function, including activation at hyperpolarized potentials, and enhanced persistent current. We hypothesize that *SCN3A* encephalopathy presents in the early infantile period due to the developmental expression pattern of *SCN3A*, combined with prominent gain-of-function effects predicted to increase neuronal excitability. We further show that the enhanced persistent current seen in mutant channels may be selectively inhibited with the antiseizure medications lacosamide and phenytoin. Given the transient developmental trajectory of *SCN3A*, it is hoped that partial normalization of pathological epilepsy-associated ion channel activity in the neonatal period in patients with *SCN3A* encephalopathy could protect the newborn brain until Nav1.3 is replaced by Nav1.1, 1.2, and 1.6, later in infancy.

Acknowledgment

This work was supported by NIH National Institute of Neurological Disorders and Stroke (K08 NS097633) and the Burroughs Wellcome Fund Career Award for Medical Scientists to E.M.G.

We thank T. Hoshi, D. Ren, and E. D. Marsh for discussions and a critical reading of the manuscript; M. Covarrubias for a tsA-201 cell line; L. L. Isom for the gift of a β-1 cDNA clone; and A. L. George for the gift of a β-2 cDNA clone.

Author Contributions

T.Z., I.H., and E.M.G., contributed to the conception and design of the study; all authors contributed to the acquisition and analysis of data; T.Z. and E.M.G. contributed to drafting the text and preparing the figures.

Potential Conflicts of Interest

Nothing to report.

References

1. Catterall WA. From ionic currents to molecular mechanisms: the structure and function of voltage-gated sodium channels. Neuron 2000;26:13–25.
2. Catterall WA. Voltage-gated sodium channels at 60: structure, function and pathophysiology. J Physiol 2012;590:2577–2589.

3. O'Malley HA, Isom LL. Sodium channel β subunits: emerging targets in channelopathies. Annu Rev Physiol 2015;77:481–504.
4. Catterall WA, Goldin AL, Waxman SG. International Union of Pharmacology. XXXIX. Compendium of voltage-gated ion channels: sodium channels. Pharmacol Rev 2003;55:575–578.
5. Claes L, Del-Favero J, Ceulemans B, et al. De novo mutations in the sodium-channel gene SCN1A cause severe myoclonic epilepsy of infancy. Am J Hum Genet 2001;68:1327–1332.
6. Claes L, Ceulemans B, Audenaert D, et al. De novo SCN1A mutations are a major cause of severe myoclonic epilepsy of infancy. Hum Mutat 2003;21:615–621.
7. Wolff M, Johannesen KM, Hedrich UBS, et al. Genetic and phenotypic heterogeneity suggest therapeutic implications in SCN2A-related disorders. Brain 2017;140:1316–1336.
8. Kearney JA, Plummer NW, Smith MR, et al. A gain-of-function mutation in the sodium channel gene Scn2a results in seizures and behavioral abnormalities. Neuroscience 2001;102:307–317.
9. Sugawara T, Tsurubuchi Y, Agarwala KL, et al. A missense mutation of the Na + channel alpha II subunit gene Na(v)1.2 in a patient with febrile and afebrile seizures causes channel dysfunction. Proc Natl Acad Sci U S A 2001;98:6384–6389.
10. Larsen J, Carvill GL, Gardella E, et al. The phenotypic spectrum of SCN8A encephalopathy. Neurology 2015;84:480–489.
11. Veeramah KR, O'Brien JE, Meisler MH, et al. De novo pathogenic SCN8A mutation identified by whole-genome sequencing of a family quartet affected by infantile epileptic encephalopathy and SUDEP. Am J Hum Genet 2012;90:502–510.
12. Cheah CS, Westenbroek RE, Roden WH, et al. Correlations in timing of sodium channel expression, epilepsy, and sudden death in Dravet syndrome. Channels 2013;7:468–472.
13. Whitaker WR, Clare JJ, Powell AJ, et al. Distribution of voltage-gated sodium channel alpha-subunit and beta-subunit mRNAs in human hippocampal formation, cortex, and cerebellum. J Comp Neurol 2000;422:123–139.
14. Beckh S, Noda M, Lübbert H, Numa S. Differential regulation of three sodium channel messenger RNAs in the rat central nervous system during development. EMBO J 1989;8:3611–3616.
15. Felts PA, Yokoyama S, Dib-Hajj S, et al. Sodium channel alpha-subunit mRNAs I, II, III, NaG, Na6 and hNE (PN1): different expression patterns in developing rat nervous system. Brain Res Mol Brain Res 1997;45:71–82.
16. Nassar MA, Baker MD, Levato A, et al. Nerve injury induces robust allodynia and ectopic discharges in Na $_{v}$1.3 null mutant mice. Mol Pain 2006;2:1733–1744.
17. Hains BC, Klein JP, Saab CY, et al. Upregulation of sodium channel Nav1.3 and functional involvement in neuronal hyperexcitability associated with central neuropathic pain after spinal cord injury. J Neurosci 2003;23:8881–8892.
18. Guo F, Yu N, Cai J-Q, et al. Voltage-gated sodium channel Nav1.1, Nav1.3 and beta1 subunit were up-regulated in the hippocampus of spontaneously epileptic rat. Brain Res Bull 2008;75: 179–187.
19. Li H-J, Wan R-P, Tang L-J, et al. Alteration of Scn3a expression is mediated via CpG methylation and MBD2 in mouse hippocampus during postnatal development and seizure condition. Biochim Biophys Acta 2015;1849:1–9.
20. Sun G, Werkman TR, Battefeld A, et al. Carbamazepine and topiramate modulation of transient and persistent sodium currents studied in HEK293 cells expressing the Na(v)1.3 alpha-subunit. Epilepsia 2007;48:774–782.
21. Estacion M, Gasser A, Dib-Hajj SD, Waxman SG. A sodium channel mutation linked to epilepsy increases ramp and persistent current of Nav1.3 and induces hyperexcitability in hippocampal neurons. Exp Neurol 2010;224:362–368.
22. Vanoye CG, Gurnett CA, Holland KD, et al. Neurobiology of disease novel SCN3A variants associated with focal epilepsy in children. Neurobiol Dis 2014;62:313–322.
23. Holland KD, Kearney JA, Glauser TA, et al. Mutation of sodium channel SCN3A in a patient with cryptogenic pediatric partial epilepsy. Neurosci Lett 2008;433:65–70.
24. Lamar T, Vanoye CG, Calhoun J, et al. SCN3A deficiency associated with increased seizure susceptibility. Neurobiol Dis 2017;102:38–48.
25. Wang Y, Du X, Bin R, et al. Genetic variants identified from epilepsy of unknown etiology in Chinese children by targeted exome sequencing. Sci Rep 2017;7:40319.
26. Sadleir LG, Mountier EI, Gill D, et al. Not all *SCN1A* epileptic encephalopathies are Dravet syndrome. Neurology 2017;89:1035–1042.
27. Chen Y-J, Shi Y-W, Xu H-Q, et al. Electrophysiological differences between the same pore region mutation in SCN1A and SCN3A. Mol Neurobiol 2015;51:1263–1270.
28. Grant AC, Vazquez B. A case of extended spectrum GEFS+. Epilepsia 2005;46(suppl 10):39–40.
29. Vanoye CG, Lossin C, Rhodes TH, George AL. Single-channel properties of human Na $_{V}$ 1.1 and mechanism of channel dysfunction in *SCN1A*-associated epilepsy. J Gen Physiol 2006;127:1–14.
30. Colombo E, Franceschetti S, Avanzini G, Mantegazza M. Phenytoin inhibits the persistent sodium current in neocortical neurons by modifying its inactivation properties. PLoS One 2013;8:e55329.
31. Crill WE. Persistent sodium current in mammalian central neurons. Annu Rev Physiol 1996;58:349–362.
32. Fleidervish IA, Friedman A, Gutnick MJ. Slow inactivation of Na + current and slow cumulative spike adaptation in mouse and guinea-pig neocortical neurones in slices. J Physiol 1996;493:83–97.
33. Stafstrom CE. Persistent sodium current and its role in epilepsy. Epilepsy Curr 2007;7:15–22.
34. Mantegazza M, Curia G, Biagini G, et al. Voltage-gated sodium channels as therapeutic targets in epilepsy and other neurological disorders. Lancet Neurol 2010;9:413–424.
35. Sheets PL, Heers C, Stoehr T, Cummins TR. Differential block of sensory neuronal voltage-gated sodium channels by lacosamide [(2R)-2-(acetylamino)-N-benzyl-3-methoxypropanamide], lidocaine, and carbamazepine. J Pharmacol Exp Ther 2008;326:89–99.
36. de Greef BTA, Merkies ISJ, Geerts M, et al. Efficacy, safety, and tolerability of lacosamide in patients with gain-of-function Nav1.7 mutation-related small fiber neuropathy: study protocol of a randomized controlled trial—the LENSS study. Trials 2016;17:306.
37. Jo S, Bean BP. Lacosamide inhibition of Nav1.7 voltage-gated sodium channels: slow binding to fast-inactivated states. Mol Pharmacol 2017;91:277–286.
38. Lampl I, Schwindt P, Crill W. Reduction of cortical pyramidal neuron excitability by the action of phenytoin on persistent Na + current. J Pharmacol Exp Ther 1998;284:228–237.
39. Trujillano D, Bertoli-Avella AM, Kumar Kandaswamy K, et al. Clinical exome sequencing: results from 2819 samples reflecting 1000 families. Eur J Hum Genet 2017;25:176–182.
40. Jamuar SS, Lam A-TN, Kircher M, et al. Somatic mutations in cerebral cortical malformations. N Engl J Med 2014;371:733–743.
41. Platzer K, Yuan H, Schütz H, et al. GRIN2B encephalopathy: novel findings on phenotype, variant clustering, functional consequences and treatment aspects. J Med Genet 2017;54:460-470.
42. Barba C, Parrini E, Coras R, et al. Co-occurring malformations of cortical development and *SCN1A* gene mutations. Epilepsia 2014; 55:1009–1019.
43. Capes DL, Goldschen-Ohm MP, Arcisio-Miranda M, et al. Domain IV voltage-sensor movement is both sufficient and rate limiting for fast inactivation in sodium channels. J Gen Physiol 2013;142:101–112.

44. Goldin AL. Mechanisms of sodium channel inactivation. Curr Opin Neurobiol 2003;13:284–290.

45. Long SB, Campbell EB, Mackinnon R. Voltage Sensor of Kv1.2: structural basis of electromechanical coupling. Science 2005;309:903–908.

46. Shen H, Zhou Q, Pan X, et al. Structure of a eukaryotic voltage-gated sodium channel at near-atomic resolution. Science 2017;355(6328).

47. Do MTH, Bean BP. Subthreshold sodium currents and pacemaking of subthalamic neurons: modulation by slow inactivation. Neuron 2003;39:109–120.

48. Stuart G. Voltage-activated sodium channels amplify inhibition in neocortical pyramidal neurons. Nat Neurosci 1999;2:144–150.

49. Lampert A, Hains BC, Waxman SG. Upregulation of persistent and ramp sodium current in dorsal horn neurons after spinal cord injury. Exp Brain Res 2006;174:660–666.

50. Cusdin FS, Nietlispach D, Maman J, et al. The sodium channel β3-subunit induces multiphasic gating in Na_V 1.3 and affects fast inactivation via distinct intracellular regions. J Biol Chem 2010; 285:33404–33412.

51. Holtkamp D, Opitz T, Niespodziany I, et al. Activity of the anticonvulsant lacosamide in experimental and human epilepsy via selective effects on slow Na+ channel inactivation. Epilepsia 2017;58:27–41.

52. Aracri P, Colombo E, Mantegazza M, et al. Layer-specific properties of the persistent sodium current in sensorimotor cortex. J Neurophysiol 2006;95:3460–3468.

53. Magistretti J, Alonso A. Biophysical properties and slow voltage-dependent inactivation of a sustained sodium current in entorhinal cortex layer-II principal neurons. J Gen Physiol 1999;114:491–509.

54. Jarecki BW, Piekarz AD, Jackson JO, Cummins TR. Human voltage-gated sodium channel mutations that cause inherited neuronal and muscle channelopathies increase resurgent sodium currents. J Clin Invest 2010;120:369–378.

55. Tang C, Zhou X, Zhang Y, et al. Synergetic action of domain II and IV underlies persistent current generation in Nav1.3 as revealed by a tarantula toxin. Sci Rep 2015;5:9241.

56. Wirrell EC, Laux L, Donner E, et al. Optimizing the Diagnosis and management of Dravet syndrome: recommendations from a North American consensus panel. Pediatr Neurol 2017;68:18–34.e3.

57. Wirrell EC. Treatment of Dravet syndrome. Can J Neurol Sci 2016;43(suppl 3):S13–S18.

58. Boerma RS, Braun KP, van de Broek MPH, et al. Remarkable phenytoin sensitivity in 4 children with SCN8A-related epilepsy: a molecular neuropharmacological approach. Neurotherapeutics 2016;13:192–197.